

INVESTIGATION OF THE SOLAR AND WIND ENERGY USAGE OF A POSITIVE ENERGY FACTORY

István Ervin Háber, István Kistelekdi, István Farkas

Original scientific paper

Very important to know at a positive-energy building in the design phase is what portion of the whole energy usage will be collected from renewable resources. In this case, at RATI Factory building in Komlo, Hungary, numerical fluid simulations (CFD) have been made to determine the heat transfer coefficients (α) for photovoltaic modules in this specific installation, and to investigate the passive ventilation, assisted by so-called Venturi-Plates. The efficiency of the natural ventilation depends on the geometrical properties (openings, Venturi-tower height, Venturi-plate design, etc.), and the photovoltaic efficiency is also influenced by air flow, since it is cooling the modules. Heat transfer at photovoltaic modules can be described among other methods, with heat resistance network. The inside of material behaviour depends on physical properties, but the heat transfer at the boundary is described by α , which hangs big rate on the air flow around the modules. These CFD simulations were validated by real wind tunnel tests, and on these pre-tests is based the ventilation control and the coming measurements in the already existing building.

Keywords: CFD, energy yield, heat transfer, passive ventilation, photovoltaic, solar energy, wind tunnel

Istraživanje uporabe sunčane energije i energije vjetra u tvornici pozitivne energije

Izvorni znanstveni članak

U zgradbi pozitivne energije u fazi projektiranja vrlo je važno znati koji će dio cijelokupne potrošnje energije biti dobiven iz obnovljivih izvora. U ovom slučaju, u izgradnji tvornice RATI u Komlu, Mađarska, provedene su numeričke simulacije fluida (CFD) kako bi se odredili koeficijenti prijelaza topline (α) za fotonaponske module u toj specifičnoj instalaciji, i provjerila pasivna ventilacija, uz pomoć tako zvanih Venturijevih ploča. Učinkovitost prirodne ventilacije ovisi o geometrijskim svojstvima (otvoreni, visina Venturi-tornja, konstrukcija Venturi-ploče itd.), a na fotonaponsku učinkovitost također utječe strujanje zraka, jer se njime hlađe moduli. Prijelaz topline fotonaponskih modula može se, između ostalih metoda, opisati mrežom otpornosti na toplinu. Ponašanje materijala iznutra ovisi o fizičkim svojstvima, ali se prijelaz topline na rubovima opisuje s α , što uvelikoj ovisi o protoku zraka oko modula. Ove su CFD simulacije potvrđene stvarnim ispitivanjima aerodinamičkih tunela te se na tim prethodnim ispitivanjima temelji reguliranje ventilacije i mjerena koja se trebaju obaviti u već postojećoj zgradi.

Ključne riječi: aerodinamički tunel, CFD, energetski prinos, fotonaponski, pasivna ventilacija, prijelaz topline, sunčana energija

1 Introduction

The increase of energy prices and the global pollution not only encourages private investors to take advantage of energy-saving technologies, but also the corporate segment. The energy balance of the buildings and the heat transfer properties in structure nodes can be calculated exactly, or specified from catalogue. The energy-efficient buildings, factories, however, in many cases use the environmental elements (wind, solar, geothermal, etc.) through unique techniques, while in this size they can be economical or for some reason are strongly required.



Figure 1 The positive energy building concept of RATI with the Venturi-plates and the PV system

RATI Ltd. Factory Building (Fig. 1) is a product of new concept of architecture called energy-design, where one of the aims is to operate a facility through economical resources. To achieve the positive energy balance at the

factory building, the placement of a number of photovoltaic modules on the façade and the roof is necessary to cover the electricity consumption of the production. About 100 kWp of PV modules were planned, and in the first phase, due to the shortage of financial resources, only 12 kWp have been made so far [1]. Based on our previous examinations the solar production data of the installed PV system will be examined, but first of all the exact efficiency of the solar cells needs to be known and its changes depending on the working temperature (which is influenced by the irradiance, environmental temperature and the wind speed), so the heat transfer coefficient will be determined using CFD [2].

At the RATI factory building, the wind energy plays an important role in the realization of passive air exchange. The intensive air exchange is an important issue in the building because of the production process (plastics industry), the development of physiological harmful gases into the atmosphere cannot be avoided, the solution to reduce the concentration is constant dilution and occasional ventilation. Three pieces of plates were placed on the towers of the building which got the name Venturi-plates, and they are responsible for inducing the chimney-like ventilation in the towers located underneath. (Fig. 2). Due to the curved plates the air speeds up, and makes a vacuum effect on the channel, which is directly connected to the production hall. The concept is unique, the Venturi-plate applied on other buildings is not known, although various wing profiles and other techniques for similar purposes can be seen [3].

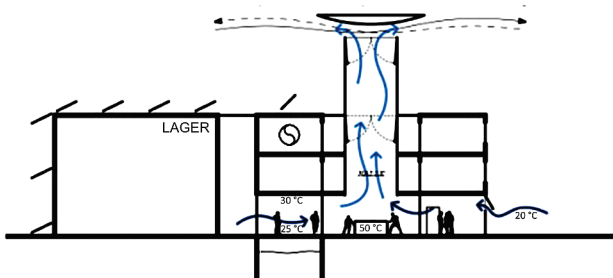


Figure 2 The estimated air flow directions in the building

Because of the Venturi plates usability issues in the first phase of the design, model of the building was placed in a wind tunnel where more variants of plates were examined and in 94 points of the building shell were measured pressure values, to make conclusions about the efficiency of ventilation.

2 Wind tunnel tests

The wind tunnel tests have been made in 2011 in the early design phase by "Gesellschaft für Aerodynamik" [4]. In the test 3 m/s inflow velocity was set in, and vortex generators and roughness elements were placed on the ground of the tunnel to simulate the natural environment. The building environment in Komlo, Hungary, can be handled as an open country from the wind profile's sight, because there are no other buildings in the neighbourhood (Fig. 3). According to this, the near surface boundary

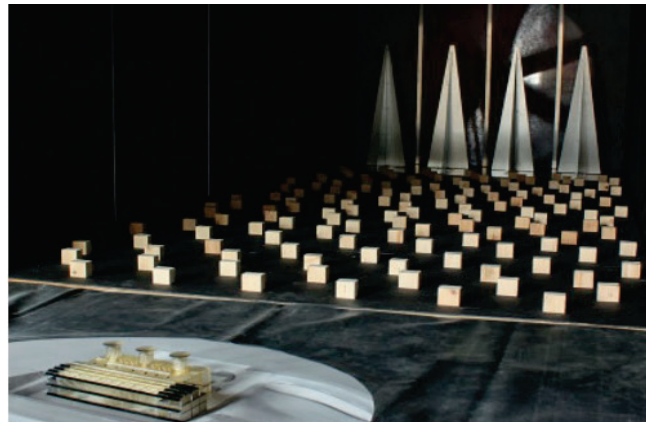


Figure 4 R ATI Building model in the wind tunnel (with vortex generators and roughness elements) and the RPT model with the reference points

Solution for four types of design in 12 different wind directions was found in the dimensionless pressure coefficients (c_p) given, calculated from the measured static pressure [7].

$$c_p = \frac{p - p_\infty}{\frac{\rho}{2} u_{in}^2}, \quad (1)$$

where p_∞ is the static pressure measured in the mean flow of the wind tunnel, p is the pressure measured on the building shell, ρ is the air density at the actual temperature, and u_{in} is the wind velocity on 10 m height (which is only 5 cm from the ground in the wind tunnel because of the dimensions).

The given pressure coefficients mean a vacuum effect if they are negative, and over pressure (inflow) if positive.

layer influences the air flow until 300 ÷ 400 meters of height [5]. In the wind tunnel it is enough to model the near surface boundary flow until 150 m height because of the dimensions of the building model (M 1:200), and this has been made by so called roughness elements in dimension of 100 × 100 mm. This type of structure of the flow and the velocity field has been described by Irwin, [6].

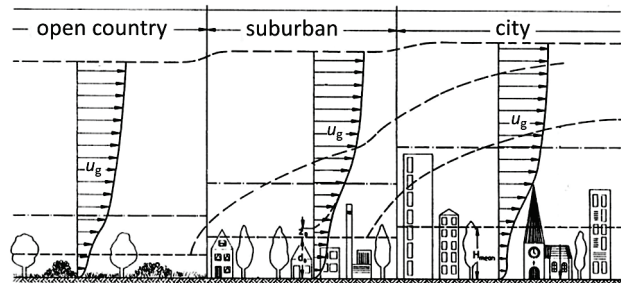


Figure 3 The wind profile in various environments [5]

The wind tunnel has a test section with 3,0 × 2,0 × 1,7 m dimensions, where the model is rotatable to set the various wind directions. Measurements were made in wind directions each 30° degree. The tests appointed to the grade of the filtration, and several types of "Venturi" constructions were investigated, to determine the best design (Fig. 4).

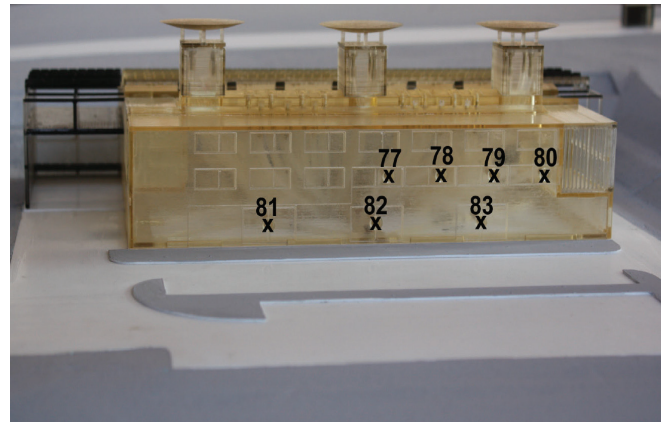


Table 1 Airflow through the towers at 30° wind direction

Tower name	Sensor number	A_{aero} / m^2	$C_{pe} - C_{pi} / -$	Airflow / m^3/h
Tower 1 West	1	1,86	-0,98	-19896
Tower 1 West	2	1,86	-0,89	-18949
Tower 1 West	3	1,86	-0,49	-14118
Tower 1 West	4	1,86	-0,6	-15588
Tower 2 Middle	5	1,86	-1,13	-21414
Tower 2 Middle	6	1,86	-0,98	-19886
Tower 2 Middle	7	1,86	-0,58	-15261
Tower 2 Middle	8	1,86	-0,56	-15114
Tower 3 East	9	1,86	-1	-20129
Tower 3 East	10	1,86	-0,94	-19496
Tower 3 East	11	1,86	-0,58	-15366
Tower 3 East	12	1,86	-0,55	-14926
Gate 1	81	12,71	0,74	73118
Gate 2	82	12,71	0,64	67931
Gate 3	83	12,71	0,66	69094

In this work only the oval type of Venturi-plates will be introduced (in which case the horizontal section of the tower is: $4,90 \times 3,80$ m), because as the result of the wind tunnel tests this type was chosen, and has been built. The wind tunnel test calculations based on the 30° wind direction were only detailed, for which $210\,143$ m^3/h flow rate has been determined, which is distributed throughout the three towers as specified in Tab. 1. Outflow occurs through the tower, the inflow is through the gates whose biggest openings are on the shell.

3 Numerical fluid simulations

The first tests were made in wind tunnel, which had a significant financial implication, which began with the 3D printing of the factory model, and continued with the measurements in wind tunnel. Since that time, however, the factory building plans have changed in many ways, such as the closed truck loading place and the atrium on the east side, and a number of smaller outer buildings were completely erased from the first plans. Due to the changes the functioning of the venturi plates had to be checked, if the air exchange rate that is not adversely affected the flow around by any changes in the geometry. These changes will be checked by CFD (Computational Fluid Dynamics), for one wind direction, reproducing the circumstances of the wind tunnel.

The single-phase flows, in the most common form can be described by 4 pieces of time and place dependent variables containing conservation. The basic equations of conservation have the advantage that the mass, momentum and energy conservation are of the same mathematical form, which is also generally well understood, they are the Navier-Stokes equations.

The Navier-Stokes (NS) Eqs. (2) describe the movement of a unit volume of liquid. It was necessary to simplify the equations, in order to facilitate the analytical solutions it counts with ideal liquid ($\mu = \text{constant}$):

$$\begin{aligned} \frac{\partial v_x}{\partial t} + v_x \frac{\partial v_x}{\partial x} + v_y \frac{\partial v_x}{\partial y} + v_z \frac{\partial v_x}{\partial z} &= \\ = g_x - \frac{1}{\rho} \frac{\partial p}{\partial x} + \nu \left(\frac{\partial^2 v_x}{\partial x^2} + \frac{\partial^2 v_x}{\partial y^2} + \frac{\partial^2 v_x}{\partial z^2} \right), \\ \frac{\partial v_y}{\partial t} + v_x \frac{\partial v_y}{\partial x} + v_y \frac{\partial v_y}{\partial y} + v_z \frac{\partial v_y}{\partial z} &= \\ = g_y - \frac{1}{\rho} \frac{\partial p}{\partial y} + \nu \left(\frac{\partial^2 v_y}{\partial x^2} + \frac{\partial^2 v_y}{\partial y^2} + \frac{\partial^2 v_y}{\partial z^2} \right), \\ \frac{\partial v_z}{\partial t} + v_x \frac{\partial v_z}{\partial x} + v_y \frac{\partial v_z}{\partial y} + v_z \frac{\partial v_z}{\partial z} &= \\ = g_z - \frac{1}{\rho} \frac{\partial p}{\partial z} + \nu \left(\frac{\partial^2 v_z}{\partial x^2} + \frac{\partial^2 v_z}{\partial y^2} + \frac{\partial^2 v_z}{\partial z^2} \right). \end{aligned} \quad (2)$$

To determine the four unknown variables (v_x , v_y , v_z and p) the fourth equation which is necessary is the continuity equation which can be written up in the next form:

$$\frac{\partial v_x}{\partial x} + \frac{\partial v_y}{\partial y} + \frac{\partial v_z}{\partial z} = 0, \quad (3)$$

$$\rho c_p \left(\frac{\partial T}{\partial x} + v \frac{\partial T}{\partial y} + v \frac{\partial T}{\partial z} \right) = k \left(\frac{\partial^2 T}{\partial x^2} + \frac{\partial^2 T}{\partial y^2} + \frac{\partial^2 T}{\partial z^2} \right). \quad (4)$$

The energy equation (4) will be extended with the linear equation of the Boussinesq approximation (5) for the determination of the density change of the air.

$$\rho = \rho_0 (1 - \beta \Delta T). \quad (5)$$

In the technical practice, there is little need to observe the changes in the flows over time, even in case of turbulent flow; the structure of the flow pattern is usually what we are interested in. In addition, this type of time-dependent description of the calculation method is very demanding and complex, so Reynolds made the deduction of the NS equations with respect to the temporal averages (average speed and average pressure). This is called the Reynolds Averaged Navier-Stokes (RANS) equations [8].

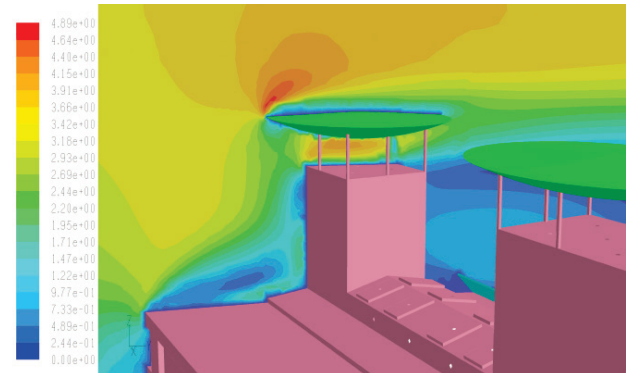


Figure 5 Velocity field calculated by CFD shown on a plane parallel to the wind direction (colormap unit: m/s)

In the simulation, several turbulence models have been examined, which can be best used to describe the flow around the building known as "blunt body" in this case. Based on the literature basically two turbulence models can be applied: the $k-\varepsilon$ and the $k-\omega$ [9].

3.1 Checking design variants of the plates with CFD

For the CFD simulation, the CAD Model (Fig. 6) of the R ATI factory was made and discretized. On the surface triangular elements were used with an average edge length of $9 \div 11$ mm. The volume mesh is based on the surface mesh so attention must be paid when making the surf mesh and must comply with the quality requirements. For example, it should not contain triangles with too sharp edges and is not permitted to sudden changes in size, or else some elements of the volume mesh could be distorted, which also affects the calculations: degrade the accuracy and destabilize the solution process (Fig. 7).

For the simulation the angle of 30° (relative to wind direction) was selected, as in this case, the mass flow rate of the air is at maximum, but as a benchmark the wind direction 120° is simulated also, because the results of the CFD calculations are closer to this. To examine the heat

transfer coefficients, 4 pcs of extra CFD calculations had to be made for various wind speeds to determine the trend of the calculated α .

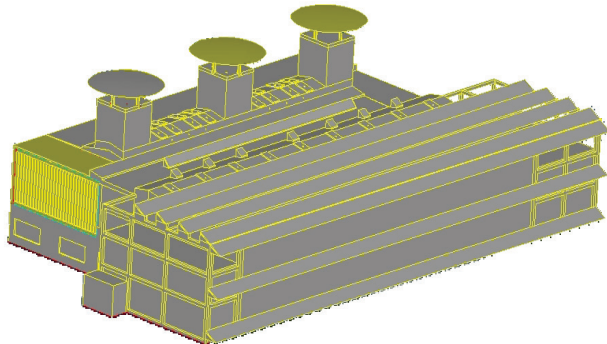


Figure 6 The CAD model of the factory for CFD

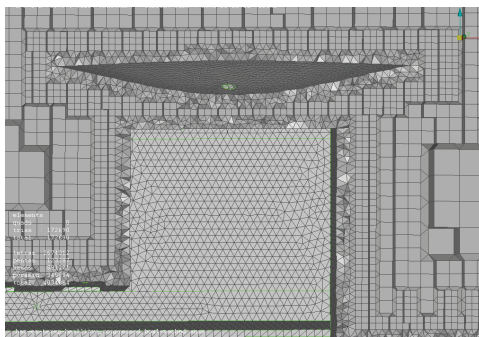


Figure 7 The CFD mesh-section at one tower

It should be also emphasized that both models (wind tunnel & CFD) can be considered as experiments; we seek the method to maximize similarity with the real circumstances. To achieve the greatest similarity there are two different ways: either the Reynolds number necessary to maintain, but in this case, because of the large difference in size it is not really possible (for the wind tunnel 66 m/s should be set according to the similarity criteria) or we can work with dimensionless pressure

coefficients which can be calculated, which is the prevailing ambient pressure independent of air velocity, such as in the automotive industry the aerodynamic drag coefficient CD. However this is defined by an empirical equation (Eq. 1.) and therefore contains substantial simplifications, which may reduce the accuracy. For these reasons, it cannot be said that the CFD calculations or wind tunnel experiments are more accurate, as with both methods it is just a try to get the highest similarity. The decision will be given by the measurements in the real building.

Despite of these, the CFD simulation and the wind tunnel test were made for the comparison with subsequent measurements, but the flow around the changed geometry has been calculated only by CFD. In addition a calculation was made in which the energy equation is solved – focusing on the exact calculation of the solar cells efficiency - but this calculation method is much closer to the real circumstances.

Fig. 8 shows that the calculated C_p values are higher for the towers in case of CFD, for the gates the values at the same points are lower, making it at the one ventilation test – when the gates and the towers are open – due to lower ΔC_p value the CFD tests define smaller volume flows. The following table shows their precise values for wind direction 30°, compared to the 120° inflow orientation.

The best results were obtained using the $k-\varepsilon$ turbulence model (in the table CFD k-E), although there were calculations performed with $k-\omega$. In the table, only the $k-\varepsilon$ and $k-\varepsilon$ NRG (with energy transport for the PV examination) values are shown, but later (in the existing building) measurements can justify the $k-\omega$ SST model also. The air speed values were also given in the cross-sections, and since in the building the air flow will be measured by heated wire anemometry, they can be used as reference. Measurements will start in the middle of 2013, in the frame of TÁMOP 4.2.1 assistance.

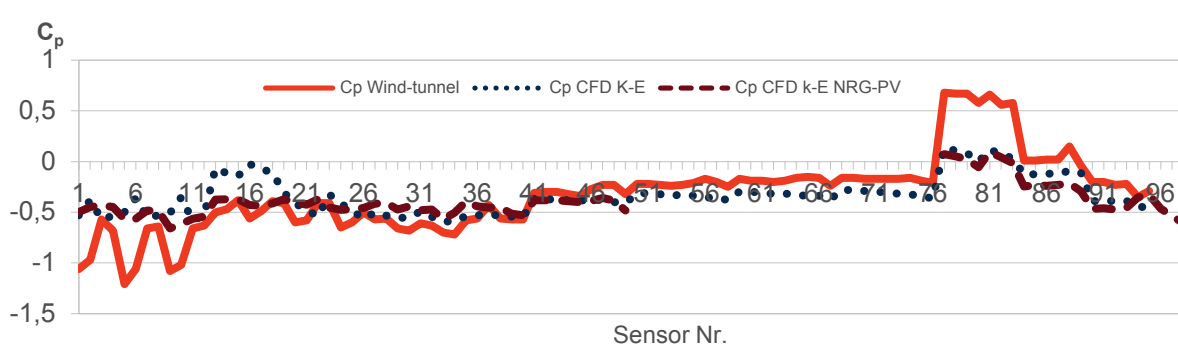


Figure 8 Comparison of the C_p values in the reference points, first line is the wind tunnel measured, the others are calculated by CFD

Table 2 Comparison of the wind-tunnel values with CFD

Tower name	Sensor Nr.	$A_{\text{aero}} / \text{m}^2$	Wind-tunnel - 30°			120°			CFD k-E - 30°			CFD k-E-NRG-PV - 30°			
			$C_{\text{pe}} - C_{\text{pi}} / -$	Airflow / m^3/h	Air speed / m/s	Airflow / m^3/h	$C_{\text{pe}} - C_{\text{pi}} / -$	Airflow / m^3/h	Air speed / m/s	$C_{\text{pe}} - C_{\text{pi}} / -$	Airflow / m^3/h	Air speed / m/s	$C_{\text{pe}} - C_{\text{pi}} / -$	Airflow / m^3/h	Air speed / m/s
Tower 1 West	1	1,86	-0,98	-19896	-2,9713	3673	-0,45	-9108,32	-1,360	-0,36	-7273,40	-1,086			
Tower 1 West	2	1,86	-0,89	-18949	-2,8299	2869	-0,30	-6442,15	-0,962	-0,32	-6882,44	-1,027			
Tower 1 West	3	1,86	-0,49	-14118	-2,1084	1839	-0,49	-14092,2	-2,104	-0,32	-9138,26	-1,364			
Tower 1 West	4	1,86	-0,6	-15588	-2,3280	9113	-0,46	-11837,1	-1,767	-0,33	-8489,56	-1,267			
Tower 2 Middle	5	1,86	-1,13	-21414	-3,1980	-3157	-0,42	-7897,78	-1,179	-0,42	-8034,99	-1,199			
Tower 2 Middle	6	1,86	-0,98	-19886	-2,9698	-2746	-0,28	-5737,63	-0,857	-0,41	-8399,01	-1,254			
Tower 2 Middle	7	1,86	-0,58	-15261	-2,2791	-1758	-0,47	-12386,4	-1,850	-0,36	-9581,82	-1,430			
Tower 2 Middle	8	1,86	-0,56	-15114	-2,2572	2572	-0,45	-12160,4	-1,816	-0,38	-10239,8	-1,529			

Table 2 Comparison of the wind-tunnel values with CFD (continuation)

Tower name	Sensor Nr.	$A_{\text{aero}} / \text{m}^2$	Wind-tunnel - 30°		120°	CFD k-E - 30°			CFD k-E-NRG-PV - 30°			
			$C_{\text{pe}} - C_{\text{pi}}$ / -	Airflow / m^3/h	Air speed / m/s	Airflow / m^3/h	$C_{\text{pe}} - C_{\text{pi}}$ / -	Airflow / m^3/h	Air speed / m/s	$C_{\text{pe}} - C_{\text{pi}}$ / -	Airflow / m^3/h	Air speed / m/s
Tower 3 East	9	1,86	-1	-20129	-3,0061	-9446	-0,43	-8629,13	-1,288	-0,49	-9812,66	-1,465
Tower 3 East	10	1,86	-0,94	-19496	-2,9116	-16431	-0,27	-5641,57	-0,842	-0,43	-8911,55	-1,330
Tower 3 East	11	1,86	-0,58	-15366	-2,2948	-11099	-0,50	-13366,8	-1,996	-0,44	-11611,1	-1,734
Tower 3 East	12	1,86	-0,55	-14926	-2,2291	-12665	-0,44	-12058,0	-1,801	-0,42	-11372,1	-1,698
Summa				-210143		-37236		-119357			-109746	
Gate 1	81	12,7	0,74	73118	1,5980	-30176	0,12	61070,81	9,120	0,22	44359,67	6,624
Gate 2	82	12,7	0,64	67931	1,4846	26555	0,08	42200,67	6,302	0,19	37371,11	5,581
Gate 3	83	12,7	0,66	69094	1,5101	40847	0,03	16086,23	2,402	0,14	28015,91	4,183
Summa				210143		37236		119357,7			109746,7	

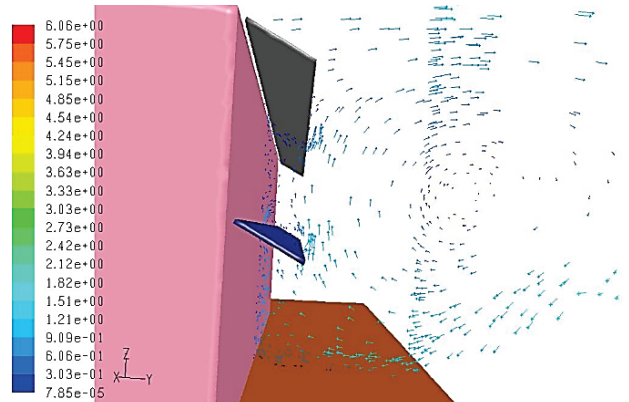
3.2 Calculation of the heat transfer coefficients for PV modules at the Factory PV plant

The efficiency of the photovoltaic modules, and therefore the power output under the same irradiation conditions, are also dependent on the PV modules' or PV cells' operating temperature. In fact the modules temperature can reach $80 \div 90^\circ\text{C}$ between naturally conditions, where the efficiency loses $20 \div 30\%$ from its originally given value. The operating temperature can be lowered by installing the modules in an appropriate way, allowing the cooling effect of natural convection flows. There are more ways to define the temperature of one PV module. Some manufacturers define a constant number (which can be replaced in the Eq. (6)), called Nominal Operating Cell Temperature (*NOCT*), on the technical sheet of a module, which can better describe the operating conditions of a module, and give the actual PV temperature. The NOCT number of a module will be determined at irradiation 800 W/m^2 , at temperature 20°C and wind velocity 1 m/s , while it is assumed that wind can flow around it

$$T_{\text{PVcell}} = T_{\text{air}} + \frac{\text{NOCT} - 20}{80} I. \quad (6)$$

Substituting the proper values in the equation, where T_{air} is the environmental temperature in $^\circ\text{C}$ and I is the irradiation in W/m^2 , the actual operating temperature of the module can be calculated. The above formula is experimental and simplified, the convection and the heat conduction are taken into consideration, but presupposes it, that the heat conduction coefficient of the substance does not change powerfully with the temperature.

To calculate the modules accurate temperature, at least the surface heat transfer coefficients (α) at various flow rates have to be determined, which defines the leaving quantity of heat from the modules. The heat transfer coefficients which will be served by the calculations, will be used at the heatflow-network model (Fig. 9) we presented in our previous works [10]. This network describes the material layer junctions of the photovoltaic module, represented with their heat resistance. This heatflow-network model was implemented in LabView, and this is a one dimension steady state model which is able to describe the junction temperatures in the photovoltaic module. With all the measured meteorological ingoing data, this model is used for photovoltaic yield-prediction.

**Figure 9** The velocity vectors at the PV modules at 3 m/s wind speed

At the defining of the boundary conditions of the equations, the physical parameters of the air are constant, except the density (5). The environmental temperature is 300 K , the temperature of the modules comes out from the radiation. At PV cells, most of the absorbed solar radiation is converted into heat, which increases the temperature of the cells. The solar heat gain by the PV modules was calculated from the insulation minus the reflection (5 %) and the energy conversion into electricity (about 15 %). A radiation model was used in the simulation case too to calculate the radiation heat losses.

In all cases five different wind speeds were examined for the heat transmission of the modules, in order $v_{\text{wind}} = \{0, 1, 3, 5, 7\} \text{ m/s}$, based on the wind speeds occurring in Hungary mostly.

Through the calculations the surface heat transfer coefficients of the photovoltaic modules have been defined in the given environment.

An average of the values was made from the calculated heat transfer coefficients, hereby the biggest deflection was 2,54 %. The linear function of the average values may be used in the heatflow network model, while its ingoing parameter is the wind velocity, which can be delivered from one of the initial values of the block oriented model.

The fitted linear equations for south Eq. (7) and north Eq. (8) wind direction:

$$\alpha_{\text{south}} = 0,9567v_{\text{wind}} + 2,4585, \quad (7)$$

$$\alpha_{\text{north}} = 1,7512v_{\text{wind}} + 3,2561. \quad (8)$$

In some cases the north and south cases can be handled separately, but in our calculations – in the heat resistance model based simulations – only the typical

installation positions are involved, and therefore an average (9) is made of the two equations of directions.

$$\alpha_{\text{avg}} = 1,35v_{\text{wind}} + 2,85. \quad (9)$$

It should be noted that the model would be more accurate if the averaging were based on the wind direction frequency. This investigation should be the next step to get the photovoltaic-yield model more precise.

Table 3 The CFD calculated heat transfer coefficients

Wind velocity, m/s	Heat transfer coefficients, W/(m ² ·K)			
	Surface average at south wind direction	Surface average at north wind direction	Linear equation made values - south	Linear equation made values - north
0	2,9	2,9	2,4585	3,2561
1	3,6	4,8	3,4152	5,0073
3	4,1	9,4	5,3286	8,5097
5	7,6	12,1	7,242	12,0121
7	9,4	15,1	9,1554	15,5145
9			11,0688	19,0169
11			12,9822	22,5193



Figure 10 The new R ATI Factory building with the 12 kWp PV plant and the Venturi-towers)

4 Conclusion

This case study is a test for an already developed algorithm, which aims mainly to photovoltaic solar yield determination, but in this case is being applied to investigate the natural ventilation in a unique system, and where the classical HVAC analysis does not work due to the specific geometrical circumstances. The towers with the Venturi-plate on top, enable to save 7025 kW·h annually, thanks to the reduced electricity costs [11].

The calculated heat transfer coefficients are used in the PV energy yield simulation [10], to determine the solar proportion in the annual electricity consumption.

Among the other techniques used at this positive energy factory, these investigations can tell what size of systems have to be used to achieve the goal – to have a real economical building like this.

Acknowledgements

This paper was funded by a grant from the SROP-4.2.2.C-11/1/KONV-2010-0005, Well-being in the Information Society research and development program.

5 References

- [1] Kistelekdi, I.; Baranyai B. Dynamic simulation supported indoor climate and energy building modeling, Proceedings of ICCEA Konferencia, 2012, Hong Kong.
- [2] Haber, I.; Farkas, I. Analysis of the air flow at photovoltaic modules for cooling purposes. // Pollack Periodica, Akademiai Kiado, Budapest. 7, (2012), pp. 113-121.
- [3] A'zami, A. Badgir in traditional Iranian architecture, Proceedings of International Conference "Passive and Low Energy Cooling for the Built Environment", Greece, 2005, pp. 1021-1026.
- [4] Bauhofer, B. Windkanalstudie RATI Kft. 2011.
- [5] Plate, E. J. Urban Climates and Urban Climatic Modelling: An Introduction, edited in Wind Climate in Cities. // Nato ASI Series E: Applied Sciences. 277, (1993), pp. 23-39.
- [6] Irwin, H. P. A. H. The design of spires for wind simulation. // Journal of Wind Engineering and Industrial Aerodynamics. 7, (1981), pp. 361-366.
- [7] Kistelekdi, I.; Baranyai, B. Windkanaluntersuchungen zwecks Quantifizierung und Validierung der Wirkung von Windinduktion und thermischen Auftriebskräften auf die natürliche Lüftung eines industriellen Innovationszentrums. // Bauphysik, Ernst & Sohn, Berlin. 35, (2012), pp. 229-237.
- [8] Moshfegh, B.; Sandberg, M. Flow and heat transfer in the air gap behind photovoltaic panels. // Renewable and Sustainable Energy Reviews. 2, (1998), pp. 287-301.
- [9] Brinkworth, B. J. Estimation of flow and heat transfer for the design of PV cooling ducts. // Solar Energy. 69, (2000), pp. 413-420.
- [10] Haber, I.; Farkas, I. Combining CFD simulations with block oriented heatflow-network model for prediction of photovoltaic energy-production. // Journal of Physics, IOP Publishing. 268, (2011), pp. 1-7.
- [11] Kistelekdi, I.; Solymosi, S. Dynamische bauklimatische und -energetische Simulationen des RATI-Gebäudekomplexes 2010–2012.

Authors' addresses

Istvan Ervin Haber, Professor Assistant

Department of Information Technology, Pollack Mihály Faculty of Engineering and Information Technology, University of Pécs
Rókus str. 2, H-7624 Pécs, Hungary
E-mail: ihaber@pmmit.pte.hu

Istvan Kistelekdi, DLA, Associate Professor

Department of Energy Design, Pollack Mihály Faculty of Engineering and Information Technology, University of Pécs
Rókus str. 2, H-7624 Pécs, Hungary
E-mail: kistelekdis@pmmit.pte.hu

Istvan Farkas, D.Sc. Full Professor

Department of Physics and Process Control, Szent István University of Gödöllő
Prater Károly str. 1, H-2034 Gödöllő, Hungary
E-mail: istvan.farkas@pmmit.pte.hu